LATVIAN JOURNAL OF PHYSICS AND TECHNICAL SCIENCES
2014, N 2

DOI: 10.2478/lpts-2014-0009

AN INDUCTION MOTOR BASED WIND TURBINE EMULATOR

A. Sokolovs[1], L. Grigans[1,2], E. Kamolins[1], J. Voitkans[1]

[1]Riga Technical University
1 Kalku Str., Riga, LV-1658, LATVIA
e-mail: Alvis.Sokolovs@rtu.lv

[2]Institute of Physical Energetics
21 Aizkraukles Str., Riga, LV-1006, LATVIA
e-mail: Linards.Grigans@gmail.com

The authors present a small-scale wind turbine emulator based on the AC drive system and discuss the methods for power coefficient calculation. In the work, the experimental set-up consisting of an AC induction motor, a frequency converter, a synchronous permanent magnet generator, a DC-DC boost converter and DC load was simulated and tested using real-life equipment. The experimentally obtained wind turbine power and torque diagrams using the emulator are in a good agreement with the theoretical ones.

Keywords: *wind turbine (WT), wind turbine emulator, wind energy conversion.*

1. INTRODUCTION

Renewable energy sources are the main topic for a few past decades, with the most rapid development of wind power systems.

In earlier works (e.g. [1-12]) the use of electric drive wind turbine emulators for simulating the torque of a wind turbine is reported.

Wind turbine emulators with variable speed drives are commonly used, since it is a cheaper and easier way to control the generator speed and power as compared with a real wind turbine. The research into electric generators, converters and control systems under laboratory conditions necessitates that there be appropriate test equipment that can simulate natural weather conditions.

In this paper, the authors present a laboratory set-up that is built for detailed research on the power converter control for a direct drive synchronous wind generator on permanent magnets. The set-up can be used for tracking the maximum power point or testing the pitch control algorithm as well as can serve the educational purposes for studying the control and dynamics of wind power systems. Also, some modifications of the set-up allow for testing the permanent magnet synchronous generators (PMSGs), synchronous generators with excitation, squirrel-cage induction generators or double-fed induction generators. In every case, a correct turbine model must be obtained and loaded into the system controller.

Further in this paper, the wind turbine emulator hardware, control program and Matlab simulation model are described and the experimental results are presented. As stated in [13], the wind turbine emulator can be used for different experiments – e.g., for studying the influence of wind shear and tower shadow on the power quality or for testing the efficiency of a new algorithm for maximum power point tracking.

2. WIND TURBINE MODEL

In general, the kinetic energy of the undisturbed upstream wind flow over a definite section with area A can be calculated as

$$P_w = \frac{1}{2} A v^3 \rho \,, \tag{1}$$

where v is the wind speed, and ρ is the density of air. In turn, the mechanical power that can be transferred from wind to the generator is

$$P_T = \frac{1}{2} A v^3 \rho C_p \,. \tag{2}$$

Here A is the area covered by the rotor blades of turbine, and C_P is the wind turbine power coefficient. Equation (2) can be rewritten in terms of the rotor radius r_{rot}:

$$P_T = \frac{1}{2} \pi r_{rot}^2 \rho v^3 C_p \,. \tag{3}$$

The aerodynamic torque of the wind turbine is also a function of wind speed v, and is calculated as

$$T_A = \frac{1}{2} \pi r^3 \rho v^2 C_T \,, \tag{4}$$

where C_T is the aerodynamic coefficient that relates to C_P by the tip speed ratio (TSR) λ:

$$C_T = \frac{C_p}{\lambda} \,. \tag{5}$$

The TSR λ is defined as the ratio of rotational speed ω of the tip of turbine rotor blade and wind speed v:

$$\lambda = \frac{\omega r}{v} \,. \tag{6}$$

Power coefficient C_P is considered the most important parameter in the power regulation of a turbine. In order to capture the maximum available power at a particular wind speed the rotational speed of the turbine rotor ω is relevant. Aerodynamic characteristics of the WT blades define the optimum rotational speed of the rotor, and any deviation from this speed causes a significant drop in the captured wind power. At the same time, the rotational speed directly depends on the generator load and wind speed variations. To calculate the power captured from wind, the power coefficient should be defined.

The power coefficient C_P is a nonlinear function of TSR λ and blade pitch angle β characterizing the aerodynamic behaviour of rotor blades. The C_P value differs for each turbine type. Since this value depends on the wind speed, it is given by turbine manufactures in the look-up tables. Theoretical models of $C_P(\lambda,\beta)$ have been developed and expressed analytically. For example, in [13] C_P calculation is done as

$$C_p(\lambda,\beta) = C_1\left(\frac{C_2}{\lambda_i} - C_3\beta - C_4\right)e^{-\frac{C_5}{\lambda_i}} + C_6\lambda\,, \tag{7}$$

with

$$\frac{1}{\lambda_i} = \frac{1}{\lambda + 0.08\beta} - \frac{0.035}{\beta^3 + 1}\,. \tag{8}$$

In (7) the C_1 through C_6 are coefficients that depend on the turbine type, with C_1 and C_6 calculated as

$$C_1 = \frac{C_p}{\left(\frac{C_2}{\lambda_i} - C_4\right)e^{-\frac{C_5}{\lambda_i}} + k\lambda}\,, \tag{9}$$

$$C_6 = k \cdot C_1\,, \tag{10}$$

and

$$k = -\left(C_2 \cdot \frac{C_5}{\lambda_i} - C_4 \cdot C_5 - C_2\right) \cdot e^{-\frac{C_5}{\lambda_i}\big/\lambda}\,. \tag{11}$$

Coefficients C_2, C_3, C_4 and C_5 are used as shown in [13].

In [14] a similar equation for C_P is presented as a function of λ and β with different coefficients:

$$C_p(\lambda,\beta) = C_1\left(\frac{C_2}{\lambda_i} - C_3\beta - C_7\beta^{C_8} - C_4\right)e^{-\frac{C_5}{\lambda_i}}\,, \tag{12}$$

where C_7 and C_8 are additional coefficients determined by the turbine type [15], and λ_i is the same as in (8). In [16] C_P is approximated with the sine wave function:

$$C_p(\lambda) = (C_1 - C_2\beta)\sin\left(\frac{\pi.(\lambda - C_3)}{C_4 - C_3\beta}\right) - C_6 \cdot (\lambda - C_7\beta)\,, \tag{13}$$

where $C_1 - C_7$ are different from those used in (7) and (12)

Theoretical C_P curves as function of λ are shown in Fig. 1. It can be seen that Eqs. (7) and (12) – lines 1 and 2, respectively, give rather close results at large λ values, though coefficients $C_1 - C_6$ in Eq.(12) are to be changed to fit the curves. In this case, C_1=0.27, C_2=150, C_4=3.35 and C_5=18. The coefficients C_3, C_7 and C_8 are not considered since β=0. Equation (12) described by line 2 gives more variance at low λ values due to the lack of term $C_6\lambda$ as compared with (7). Approximation (13) characterized by curve 3 has a significant deviation at higher λ values and the beginning of the curve is linearized, which gives a considerable error at low λ values.

For further calculations and C_P modelling of the wind turbine Eq. (7) will be used.

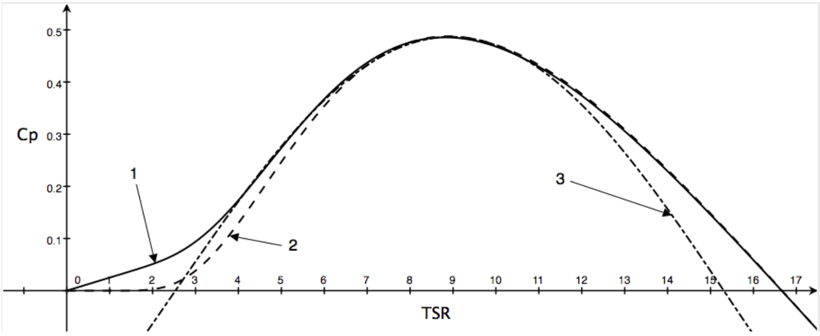

Fig. 1. Theoretical power coefficient curves 1, 2, and 3
of a wind turbine vs. λ (TSR) calculated by Eq. (7), Eq.(12), and Eq.(13), respectively.

Based on the C_P curves, the turbine power *Pt* and torque *Tt* curves are obtained as functions of the rotational speed of the rotor at different wind speed values (Fig. 2). As can be seen from (6), for the turbine to operate at maximum power coefficient the rotational speed must be proportional to the wind speed. This can be achieved when in a variable speed turbine the maximum power point tracking strategy is applied. In Fig. 2*a* it is seen that for each wind speed there is a rotational speed of the rotor that allows operation at maximum power. In (2) it is defined that the turbine power is proportional to the cube of the wind speed. Since the rotational speed of the turbine is proportional to the wind speed, the power of turbine is also proportional to the cube of rotational speed of the rotor, i.e.:

$$P_{T_{max}} = k\omega^3 . \quad (14)$$

To obtain optimal operation, torque (14) is divided by rotational speed of the rotor:

$$T_{T_{opt}} = k\omega^2 . \quad (15)$$

The maximum power and the optimum torque curves are presented in Fig. 2.

It is worth mentioning that if C_P is calculated by (12), the obtained power and torque curves (Fig. 2*a* and *b*, dashed lines) are inaccurate for several reasons: first, at low rotor speeds the turbine would not produce any power and torque even at significant wind speeds. Second, the power and torque curves for different wind speeds intersect, so that at low rotor speeds a higher wind speed produces smaller power and torque. These drawbacks should be taken into account when a wind turbine is simulated, otherwise a more precise emulator is needed. Therefore, it is recommended to use (7) for C_P calculations.

a)
b)
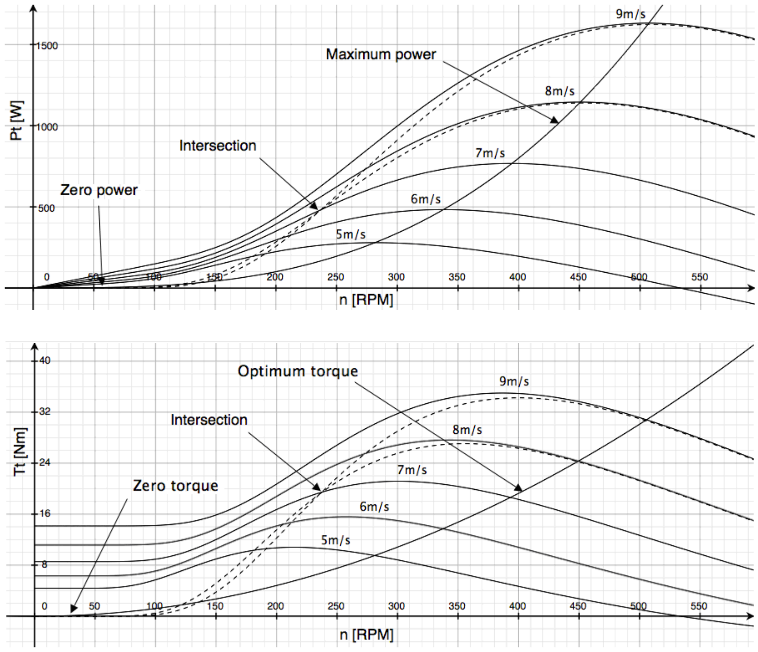

Fig. 2. Theoretical power (a) and torque (b) curves of a wind turbine as functions of rotational speed of rotor. Solid lines correspond to Eq. (7) and dashed lines – to Eq. (12).

Next, the dynamical behaviour of a wind turbine is considered. In general, the WT rotational speed variation rate is determined by the total system inertia and turbine torque. The total dynamic torque can be expressed as

$$J_S \frac{d\omega}{dt} = T_T - T_G - B_T\omega \; J_S \frac{d\omega}{dt} = T_T - T_G - B_T\omega , \tag{16}$$

where J_S is the total moment of inertia of the system,
T_G is the electromagnetic torque of generator,
B_T is the friction coefficient of turbine (in direct drive turbines may be neglected).

The total system's inertia is the sum of wind turbine inertia J_T, generator rotor inertia J_G and shaft inertia J_{sh}:

$$J_S = J_T + J_G + J_{sh} . \tag{17}$$

In the case of cylindrical shapes (the generator shaft and the rotor) the approximate moment of inertia can be calculated as

$$J = \frac{1}{2} mr^2 , \tag{18}$$

where m, r is the rotor (or shaft) mass and radius, respectively.

The moment of inertia of wind turbine blades (assuming that these are homogeneous bars) for a three-blade horizontal axis turbine can be calculated as

$$J = 3 \cdot \left(\frac{1}{3} m_b l^2 \right) = m_b l^2 , \tag{19}$$

where m_b is the mass of a rotor blade, and l is its length.

To achieve a more precise emulation of the wind turbine, its inertia and that of the whole emulator (i.e. the moment of inertia of induction motor J_{IM}) are to be taken into account. Therefore, the difference should be found between these moments of inertia:

$$\Delta J = J_T - J_{IM}\,, \qquad (20)$$

which is the virtual part of the WT moment of inertia included in the reference torque calculations.

3. SIMULINK WT MODEL

In this study, a simulation model in Simulink was developed to compare the wind turbine emulator and the Simulink WT models.

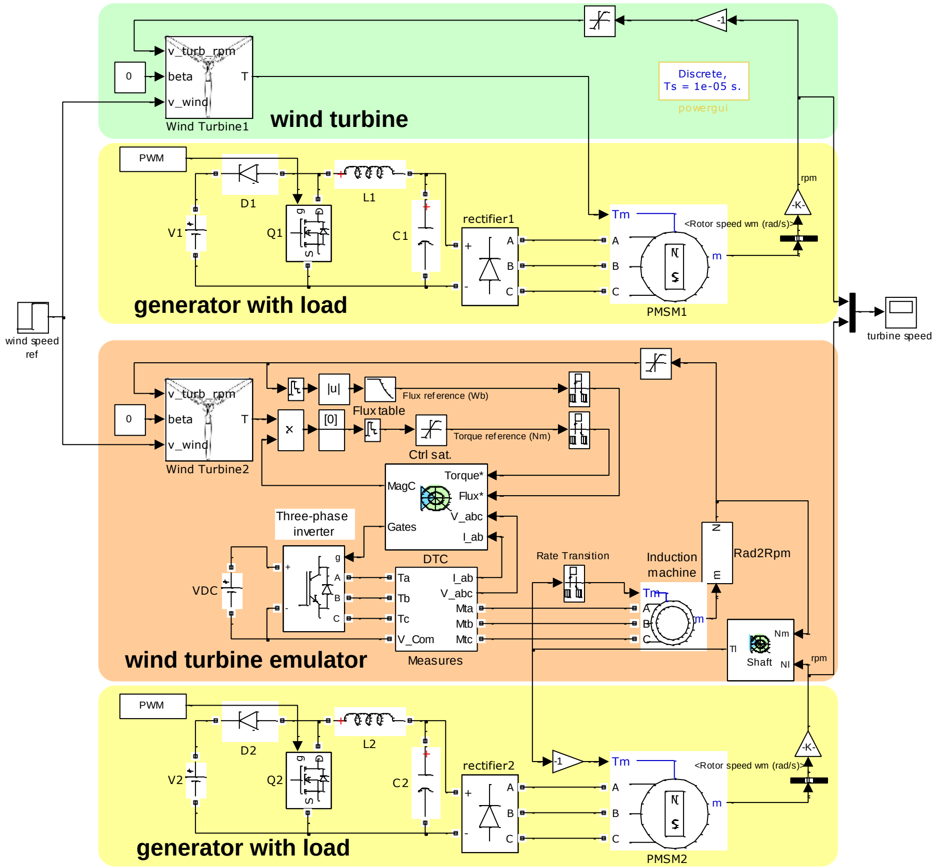

Fig. 3. Simulink WT model and the wind turbine emulator model with the same generator-load system.

Both the models contain the PMSG with a rectifier and a boost converter to 300V DC grid (Fig. 3 "generator with load"). In this figure Simulink wind turbine model is represented by Wind Turbine1 block, which calculates C_P by (7) and the turbine torque by (4) and contains the dynamic part of a wind turbine. In the emulator the same WT model is used to obtain the reference torque for frequency converter (in Fig. 3 represented by three-phase-inverter and direct torque control (DTC) units.

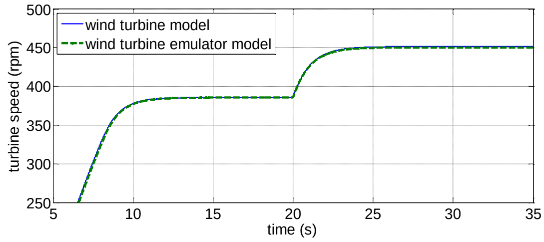

Fig. 4. Matlab simulation results for the wind turbine and its emulator models at wind speed step response from 6 to 8 m/s.

Figure 4 shows comparative simulation results for turbine dynamic response at wind speed change from 6 m/s to 8 m/s. As can be seen, the results for the wind turbine output power and torque are the same, with a negligible deviation that might arise due to losses in the AC drive system.

4. WIND TURBINE EMULATOR

A WT emulator laboratory set-up (Fig. 5) is based on a commercial 1500 rpm 7.5 kW AC induction motor with a frequency converter which implements direct torque control (DTC) algorithm. As the microcontroller, a *PIC32MX360F512L* on *EXPLORER16* development board is used, with an additional digital-analog converter for the torque reference input to the frequency converter. The rotational speed and torque are measured by on-shaft *DRBK-100* torque transducer.

a)

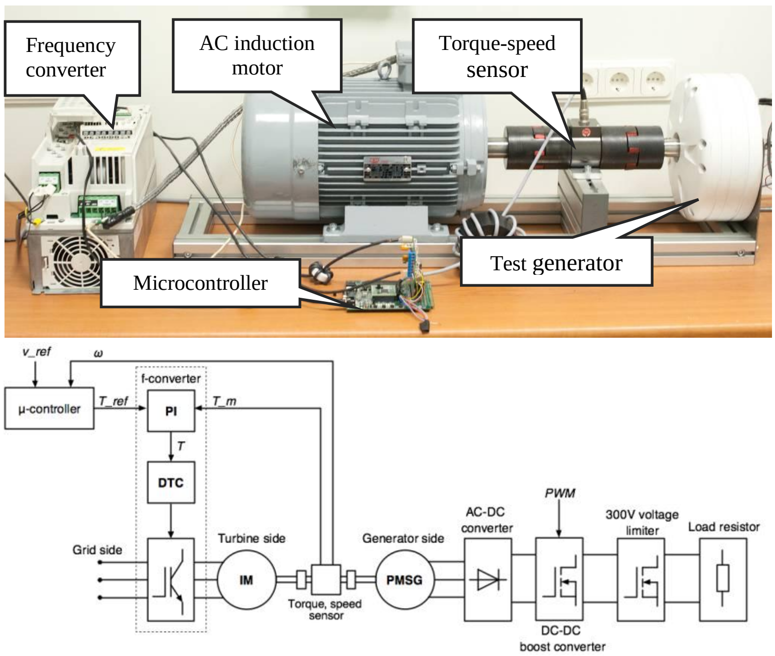

b)

Fig. 5. Wind turbine emulator: a) laboratory set-up; b) schematic diagram.

The wind speed and rotor speed ω are fed to a microcontroller in which the reference torque is calculated by Eqs. (3), (4), (6) and (7). In the case of a fixed blade (stall-controlled) turbine the pitch angle of the blade is fixed to 0^o, and, therefore the power coefficient depends only on λ; hence (7) and (8) can be simplified:

$$C_p(\lambda) = C_1\left(\frac{C_2}{\lambda_i} - C_4\right)e^{-\frac{C_5}{\lambda_i}} + C_6\lambda\,, \tag{21}$$

$$\frac{1}{\lambda_i} = \frac{1}{\lambda} - 0.035\,. \tag{22}$$

Values of coefficients $C_1 - C_6$ are mentioned before and are the same as in simulation, so that maximum C_P corresponds to nominal λ for the generator speed of 450 rpm and the rated wind speed of 8 m/s. The rotor diameter is assumed to be 3 m.

The control of wind speed is done from the user interface of the microcontroller. It is also possible to feed in a particular wind speed pattern from other sources.

5. RESULTS AND DISCUSSION

Using the WT emulator set-up (Fig. 5) the power and torque diagrams have been obtained. A schematic diagram of Fig. 5*b* provides details of the experimental set-up: on the left, the wind turbine emulator is shown as consisting of the frequency converter (f-converter), AC induction motor (IM), microcontroller (μ-controller) and torque & speed sensor. The load shown on the right consists of a PMSG (rated power 1 kW, rated speed 450 rpm), a diode rectifier (AC-DC converter), a boost DC-DC converter, a voltage limiter to 300V, and a load resistor.

The load on the generator and hence the speed of the turbine is controlled by controlling the voltage at the rectifier output. It is done by changing the duty cycle *D* of the boost converter (PWM). Since the output voltage is fixed by the voltage limiter, the input voltage is proportional to *1-D.*

By changing *D* from 0 to 1, the programmed WT torque diagrams are measured and corresponding power diagrams are calculated. In Fig. 6 the obtained power and torque diagrams are compared with the theoretical ones. It can be seen that the former are in good agreement with the latter.

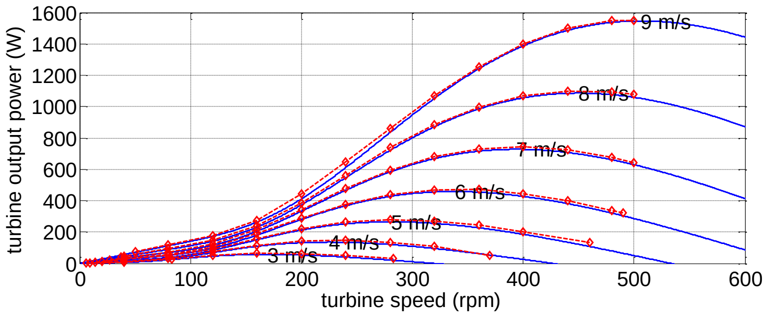

a)

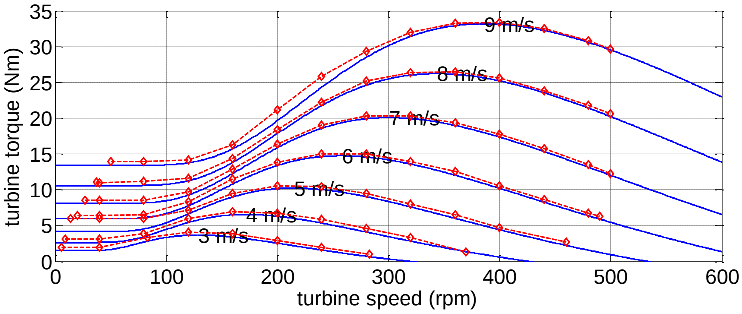

b)

Fig. 6. Experimental (dashed lines) and theoretical (solid lines) results: turbine power (a) and torque (b) *vs*. turbine speed at different wind speeds.

6. CONCLUSIONS

From the results of work the following conclusions can be drawn:

1. To obtain reliable results for the turbine output power and torque the WT power coefficient C_P should be calculated by Eq. (7).

2. The power and torque diagrams obtained with the WT emulator simulation model in Matlab Simulink and experimentally are in a good agreement (with a negligible error).

3. The WT emulator built for the research (in particular, for experiments with wind generators and wind generator control in a controlled environment) has shown a good performance. Our emulator set-up contains the elements (such as AC induction motor with frequency converter, PIC microcontroller and torque-speed on-shaft sensor) that altogether allow modelling of the wind turbine output torque taking into account the WT dynamics in the same way as under real-life conditions.

4. Depending on the microcontroller code, both stall- and pitch-controlled wind turbines can be emulated.

5. Using a WT emulator, the algorithms of maximum power point tracking can be tested.

ACKNOWLEDGMENTS

This work was supported by the European Regional Development Fund project "Development of a slow-speed power generator for wind turbines", No. 2010/0215/2DP/ 2.1.1.1.0/10/APIA/VIAA/039

REFERENCES

1. Kana, C. L., Thamodharan, M., & Wolf, A. (2001). System management of a wind-energy converter. *IEEE Transactions on Power Electronics, 16*(3), 375–381. doi:10.1109/63.923770
2. Lu, H.-C., & Chang-Chien, L.-R. (2010). Use of wind turbine emulator for the WECS development. *In: International Power Electronics Conference (IPEC)*, (pp. 3188–3195).
3. Monfared, M., Madadi Kojabadi, H., & Rastegar, H. (2008). Static and dynamic wind turbine simulator using a converter controlled dc motor. *Renewable Energy*, 33(5), 906–913.

4. Abo-Khalil, A. G. (2011). A new wind turbine simulator using a squirrel-cage motor for wind power generation systems. In *IEEE Ninth International Conference on Power Electronics and Drive Systems (PEDS)*, 750–755.
5. Voltolini, H., Granza, M. H., Ivanqui, J., & Carlson, R. (2012). Modeling and simulation of the Wind Turbine Emulator using induction motor driven by torque control inverter. *In: 10th IEEE/IAS International Conference on Industry Applications (INDUSCON),* 1–6.
6. Chinchilla, M., Arnaltes, S., & Rodriguez-Amenedo, J. L. (2004). Laboratory set-up for wind turbine emulation. *In: IEEE International Conference on Industrial Technology, IEEE ICIT'04.*, *1*, 553–557.
7. Vaheeshan, J., Vihirthanath, V., Abeyaratne, S. G., Atputharajah, A., & Ramatharan, G. (2011). Wind Turbine Emulator. *In: 6th IEEE International Conference on Industrial and Information Systems (ICIIS)*, 511–516.
8. Kumsup, S., & Tarasantisuk, C. (2010). Real-time wind turbine emulator for testing wind energy conversion systems. *In: IEEE International Energy Conference and Exhibition (EnergyCon)*, 7–9.
9. Arifujjaman, M., Iqbal, M. T., & Quaicoe, J. E. (2006). An isolated small wind turbine emulator. *Canadian Conference on Electrical and Computer Engineering, 2006. CCECE'06.*, 1854–1857
10. Neammanee, B., Sirisumrannukul, S., & Chatratana, S. (2007). Development of a wind turbine simulator for wind generator testing. *International Energy Journal, 8*(1), 21–28.
11. Cutululis, N. A., Ciobotaru, M., Ceanga, E., & Rosu, M. E. (2002). Real time wind turbine simulator based on frequency controlled AC servomotor. *Annals of "Dunarea de Jos" University of Galati, 3*, 97–101.
12. Kojabadi, H. M., Chang, L., & Boutot, T. (2004). Development of a novel wind turbine simulator for wind energy conversion systems using an inverter-controlled induction motor. *IEEE Transactions on Energy Conversion, 19*(3), 547–552.
13. Heier, S. (1998). *Grid Integration of Wind Energy Conversion Systems. Wiley & Sons*.
14. Ofualagba, G., & Ubeku, E. (2012). The modeling and dynamic characteristics of a variable speed wind turbine. *Journal of Energy Technologies and Policy, 1*(3), 10–21.
15. Manyonge, A. W., Ochieng, R. M., Onyango, F. N., & Shichikha, J. M. (2012). Mathematical modelling of wind turbine in a wind energy conversion system: Power coefficient analysis. *Applied Mathematical Sciences, 6*(91), 4527–4536.
16. Tahar, M., & Lachguer, N. (2012). Matlab Simulink as Simulation Tool for Wind Generation Systems Based on Doubly Fed Induction Machines. *In; V. Katsikis (Ed.), MATLAB - A Fundamental Tool for Scientific Computing and Engineering Applications - Vol 2*. InTech.

UZ ASINHRONĀ ELEKTRODZINĒJA BĀZES VEIDOTS VĒJA TURBĪNAS EMULATORS

A. Sokolovs, L. Grigāns, E. Kamoliņš, J. Voitkāns

K o p s a v i l k u m s

Šajā rakstā parādīta mazas jaudas vēja turbīnas emulatora izveide ar maiņstrāvas piedziņas sistēmu, kā arī analizētas vairākas turbīnas jaudas koeficienta analītiskās aprēķina metodes. Vēja turbīnas emulatora eksperimentālais stends, kas sastāv no asinhronā elektromotora, frekvenču pārveidotāja, sinhronā pastāvīgo magnētu ģeneratora, līdzstrāvas paaugstinošā pārveidotāja un slodzes,

tika pārbaudīts gan simulēšanas vidē, gan uz reālām iekārtām. Eksperimentāli iegūtās vēja turbīnas emulatora jaudas un momenta diagrammas ir salīdzinātas ar teorētiskajām.

27.02.2014.